NISTIR 6357

NEW FLAME RETARDANTS CONSORTIUM: FINAL REPORT
Flame Retardant Mechanism of Silica

Jeffrey W. Gilman, Takashi Kashiwagi, Marc Nyden, and Richard H. Harris, Jr.

United States Department of Commerce
Technology Administration
National Institute of Standards and Technology

NISTIR 6357

NEW FLAME RETARDANTS CONSORTIUM: FINAL REPORT

Flame Retardant Mechanism of Silica

Jeffrey W. Gilman, Takashi Kashiwagi, Marc Nyden,
and Richard H. Harris, Jr.
Building and Fire Research Laboratory
National Institute of Standards and Technology
Gaithersburg, MD

June 1999

U.S. Department of Commerce
William M. Daley, *Secretary*
Technology Administration
Gary Bachula, *Acting Under Secretary for Technology*
National Institute of Standards and Technology
Raymond G. Kammer, *Director*

NISTIR

NEW FLAME RETARDANTS CONSORTIUM: FINAL REPORT

Flame Retardant Mechanism of Silica

Jeffrey W. Gilman, Takashi Kashiwagi, Marc Nyden,
and Richard H. Harris, Jr.
Building and Fire Research Laboratory
National Institute of Standards and Technology
Gaithersburg, MD

June 1999

U.S. Department of Commerce
William M. Daley, *Secretary*
Technology Administration
Gary Bachula, *Acting Under Secretary for Technology*
National Institute of Standards and Technology
Raymond G. Kammer, *Director*

LIST OF TABLES

LIST OF FIGURES

New Flame Retardants Consortium: Final Report
Flame Retardant Mechanism of Silica

Jeffrey W. Gilman, Takashi Kashiwagi, Marc Nyden, Richard H. Harris, Jr.
National Institute of Standards and Technology[ψ]
Gaithersburg, MD 20899-8652, USA

ABSTRACT

The results of a two year research project carried out with the "New Flame Retardants Consortium" are reported. This investigation into the flame retardant mechanism of silica gel and other forms of silica has determined that the silica FR mechanism is comprised of two main effects. The first is a reduction in the transport rate of the thermal degradation products by dramatically increasing the viscosity of the polymer melt due to hydrogen bonding of surface silanol groups and entanglement of polymer chains within the large pores of silica gel. Second is the reduction in thermal diffusivity of the sample near the surface due to gradual accumulation of silica, which acts as a thermal insulation layer.

1. INTRODUCTION

Because of the international pressure to develop non-halogenated flame retardants a new class of flame retardants has emerged based on silicon. This is evidenced by the number of recent patents and publications where a flame retardant effect is derived from one type of silicon or another.[1] Previously, we reported on the use of silica gel combined with potassium carbonate as a new flame retardant approach, effective in polypropylene (PP), nylon 6, 6, polymethylmethacrylate (PMMA), cellulose, poly (vinyl-alcohol) (PVA), and to a lesser extent in polystyrene (PS) and poly (styrene-acrylonitrile) (SAN). The peak heat release rate was reduced by up to 68 %, with a mass fraction of 10 % additives.[2] As part of our effort to determine the flame retardant mechanism, we first focused our efforts on characterizing the char structure, which resulted from burning poly (vinyl alcohol) with these additives. We found that the additives increased the (carbonaceous) char yield, but did not change the chemical structure of the char.[3] Next, we focused our efforts on determining the affect silica material properties had on polymer flammability. As a result of these studies, we propose a general flame retardant mechanism for silica in a variety of polymers. This is based on our investigation of the effect of silica: morphology, pore volume, particle size, and silanol concentration, on the flammability and pyrolysis behavior of PP and poly (ethylene-co-vinyl acetate), EVA.

2. EXPERIMENTAL

2.1 Silica Gel –Polypropylene Study.

Experimental Design and Compounding.

A full factorial design-of-experiment, with two blocks and one center point per block, was used to evaluate the effect of three silica gel material characteristics: pore volume, particle size and surface silanol concentration [OH], and the effect of K_2CO_3. Two blocks were used to allow for the two days required for compounding the 18 samples. One to 1.5 kg of each formulation was prepared. Table 1 shows the formulations prepared, and the characteristics of the silica gels that were employed. Silica gel was used in all formulations at a mass fraction of 10%.

The silica gels were prepared, and ground to specific particle sizes, by PQ Corporation[ϖ]. The heat treatment, or calcining, of the silica gels was done at NIST. The heat treatments were done in air, at different temperatures to yield different surface silanol concentrations [OH]. The higher the temperature the lower the [OH]. The temperatures used (220 °C, 550 °C, 900 °C) were expected to yield 1.7 mmol/g, 1.0 mmol/g, and 0.5 mmol/g of SiOH respectively. At each calcining temperature the silica gel was heated until it reached a constant mass. Table 2 shows the material properties for the silica gels used.

The PP used was 95% isotactic and had a melt index of 4 g/600 s, Mw^4 ~300K, Mn ~ 90K and was purchased from General Polymers.

The dispersing agent used was polypropylene-graft-maleic anhydride (PP-g-MA) with a mass fraction of 0.6 % maleic anhydride. The PP-g-MA had a melt index of 115 g/600 s, Mw ~ 10K, Mn ~ 5K and was purchased from Aldrich. In order to determine the appropriate level of dispersing agent, (PP-g-MA), preliminary PP/PP-g-MA/silica gel formulations were compounded. We used silica gels with two different average particle sizes (7 μm and 33 μm) and two levels of PP-g-MA (mass fractions of 1 % and 5 %). The PP-g-MA was expected to aid in dispersing the silica gel in the PP by reaction of the anhydride with the surface SiOH groups as shown in scheme 1. Scanning electron microscopy, SEM, taken of the two PP/PP-g-MA/silica gel formulations with only a mass fraction of 1 % PP-g-MA showed a qualitative difference between the samples. The sample with the smaller (7 μm) particle size silica gel was not as well dispersed as the larger (33 mm) particle size silica gel. Therefore, all formulations, used for the full-factorial experimental design study, used a mass fraction of 5 % of the PP-g-MA dispersing agent, to fully disperse the smaller particle–size silica gels.

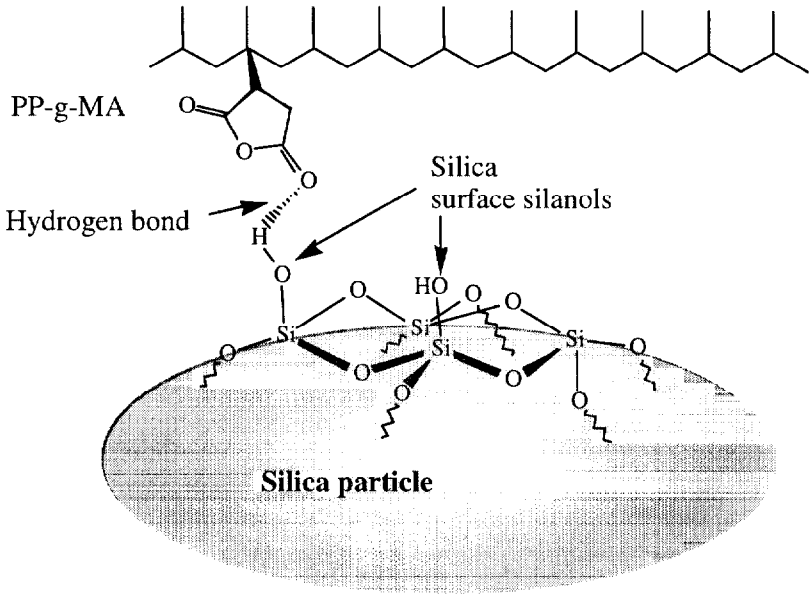

Figure 1. Hydrogen bonding between PP-g-MA and silica gel surface silanol.

Each formulation was first compounded at FMC Corporation on a conical, twin screw extruder. The extruded samples were cooled in water bath as they exited the extruder, were pelletized, and shipped to NIST. The samples were then dried at 60 °C for 24 h, in a forced air convection oven, and then in vacuo at 80 °C, for 12 h, over P_2O_5. The runs with silica gel with very low bulk density (pore volume: 3 cm^3/g) required a second compounding to obtain a homogeneous mix, therefore, all formulations were re-extruded at NIST on a Haake twin screw extruder.

ϖ Certain commercial equipment, instruments, materials, services or companies are identified in this paper in order to specify adequately the experimental procedure. This in no way implies endorsement or recommendation by NIST.

Table 1. Full-factorial experimental design for PP/silica gel formulations.

Block	Pattern[A]	PP (mass fraction %)	PP-g-MA (mass fraction %)	K_2CO_3 (mass fraction %)	Silica gel particle size (μm)	Silica gel Pore volume (cm^3/g)	Silica gel Heat treatment (°C)
2	----	85	5	0	5	0.45	220
1	---+	85	5	0	5	0.45	900
1	--+-	85	5	0	5	3.0	220
2	--++	85	5	0	5	3.0	900
1	-+--	85	5	0	20	0.45	220
2	-+-+	85	5	0	20	0.45	900
2	-++-	85	5	0	20	3	220
1	-+++	85	5	0	20	3	900
1	+---	80	5	5	5	0.45	220
2	+--+	80	5	5	5	0.45	900
2	+-+-	80	5	5	5	3.0	220
1	+-++	80	5	5	5	3.0	900
2	++--	80	5	5	20	0.45	220
1	++-+	80	5	5	20	0.45	900
1	+++-	80	5	5	20	3	220
2	++++	80	5	5	20	3	900
1	0	82.5	5	2.5	10	1.3	550
2	0	82.5	5	2.5	10	1.3	550

A: minus (-) and plus (+) indicate low or high setting respectively, while zero (0) indicates center point setting for each variable in the design formulation, e.g., (+++) = (5% K_2CCO_3, 20 μm particle size silica gel, 3 cm^3/g pore volume silica gel, 900 °C heat treatment of silica gel)

Table 2. Silica gel material properties.

Pore Volume (cm^3/g)	Particle Size (μm)	Pore Diameter (nm)	Surface Area (m^2/g)	Silanol Concentration (mmol/g)	Heat Treatment (°C)
3.0	20	28	400	0.5	900
3.0	20	28	400	1.7	220
3.0	5	28	400	0.5	900
3.0	5	28	400	1.7	220
1.3	10	15	350	1.0	500
0.45	20	2.3	800	0.5	900
0.45	20	2.3	800	1.7	220
0.45	5	2.3	800	0.5	900
0.45	5	2.3	800	1.7	220

Samples for Cone Calorimeter testing were prepared as follows. The formulated samples were extruded directly into 75 mm wide by 3 mm to 4 mm thick sheets during the second extrusion. This was done by using a heated slit die attached to the Haake extruder. These sheets were cut into ~18 g samples (~75 mm x 75 mm). Some of the samples contained bubbles, because the drying procedure did not completely remove residual water.[5] The flammability properties of the above samples were evaluated using the Cone Calorimeter with a incident heat flux of 35 kW/m^6 . Each Cone test was run three times and the results averaged. The standard deviations shown in the bar graph plots (Figure 3 to Figure 7) are a measure of the uncertainty in the Cone data. The center-point formulation was prepared two times so this gives an estimate of the batch-to-batch uncertainty combined with the Cone data repeatability. The standard deviation for the center point runs is also shown in Figure 3 through Figure 7. It should be noted that, since

the two center point formulations were prepared on different days, this standard deviation also includes the day-to-day variability.

For all other Cone Calorimeter data the uncertainties are based on the statistics derived from 3 replicate runs of several representative samples. Peak heat release rate, mass loss rate and specific extinction area (SEA) data, measured at 35 kW/m^2, were reproducible to within ± 10 % (1 σ). The carbon monoxide and heat of combustion data were reproducible to within ± 10 % (1 σ). The typical uncertainty in the HRR of one of the formulations is shown in each plot as a single error bar on the HRR curve (e.g., Figure 8).

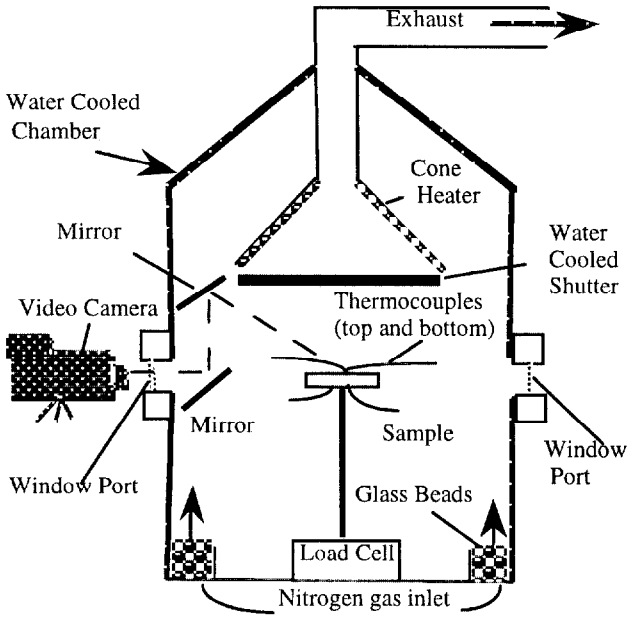

Figure 2. Schematic of Gasification device. The Gasification device allows pyrolysis, in a nitrogen atmosphere, of samples identical to those used in the Cone Calorimeter, without complications from gas phase combustion, such as heat feedback and obscuration of the sample surface from the flame.

The ethylene vinyl alcohol copolymer, EVA, used contains a mass fraction of 19 % vinyl acetate. EVA was compounded with several additives: silica gel fused silica, silica gel with K_2CO_3, and silica gel with melamine polyphosphate. The samples were compounded using a mixing roller at Sekisui Chemical Co., and all Cone samples were made by compression molding. The size of the samples was 10 cm x 10 cm x 0.3 cm thick.

2.2 Gasification Experiments.

The gasification device built at NIST is shown schematically in Figure 2. The cylindrical chamber is 0.61 m in diameter and 1.70 m in height. Two windows provide optical access. The chamber walls are water cooled to 25 °C. Products and ambient gases are removed via an exhaust duct, and a constant nitrogen flow of 7.67 L/s at 25 °C is maintained during the experiments. The temperature of the elements in the cone-shaped heater is fixed at 808 °C to maintain a constant emission spectrum for all tests. The incident radiant flux to the sample was varied by changing the distance between the sample and heater. A water-cooled shutter was extended to protect the sample from the incident radiant flux prior to testing. Flux levels varied about 8 % -10 % across 0.1 m diameter sample region. The sample, 75 mm in diameter and 8 mm in thickness, was placed in an aluminum foil pan having nearly the same diameter as that of the sample, and 13 mm high side walls. The sample mass was measured by a load cell; these data were recorded at 0.5 s intervals. The uncertainty in the measurement of interest in the gasification data is shown in each plot as an error bar. PP/silica gasification samples were made by compression molding at NIST. Table 3 shows the material properties of the four different silica samples used: a large pore volume (3 cm^3/g) silica gel (PQ Corporation), a fused silica (Siltex 44C, Kaopolite Inc., 99.5% silica), a hydrophilic fumed silica (Cabosil MS –75),

and a hydrophobic fumed silica (Wacker HDK H 2000). Ethylene vinyl acetate (19 % vinyl acetate) copolymer formulations were also evaluated in the gasification apparatus. The samples were prepared at Sekisui Chemical Co. and all samples were made by compression molding after using a mixing roller. The size of the samples was 10 cm x 10 cm x 0.3 cm thickness.

3. RESULTS and DISCUSSION

3.1 Cone Calorimetry- Silica Gel / Polypropylene Study

Figure 3 shows the plot of peak heat release rate, HRR, for four different combinations of silica gel (two particle sizes) combined with K_2CO_3 (two mass fractions), and a combination which represents a center-point formulation. Neither the silica gel particle size, nor the presence of K_2CO_3 significantly change the effect on HRR that the silica gel produces in PP. That is, each of these formulations reduces the HRR by about the same amount: about 50 %.[2] Figure 4, which shows peak HRR for combinations of silica gel pore volume and particle size, reveals that the formulations with silica gels with the highest pore volume (3 cm^3/g) have a significantly lower flammability.

It should be noted that no significant differences were observed in ignition times (42 s ± 10 s) for any of the formulations.

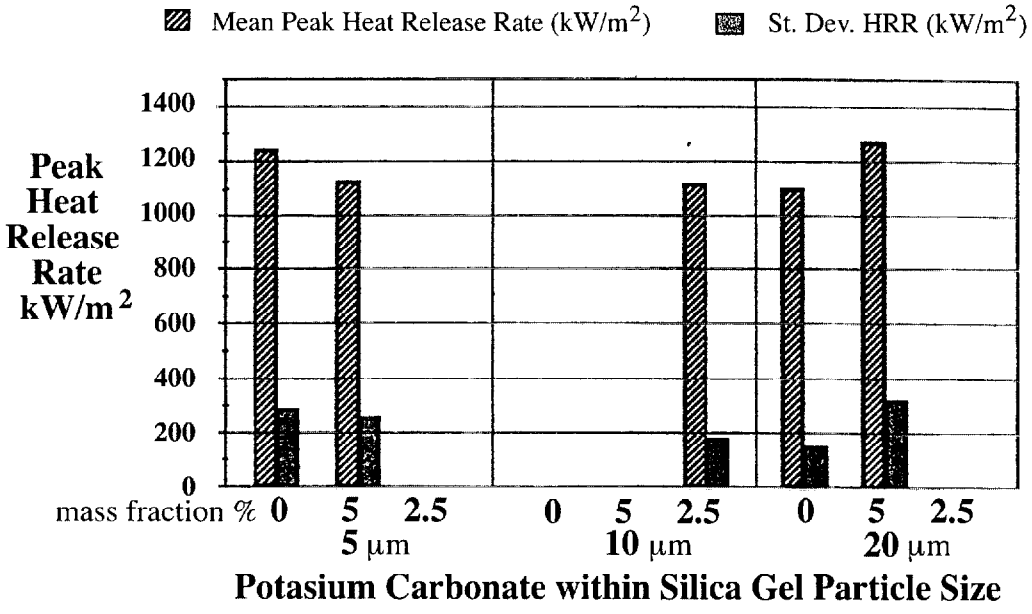

Figure 3. Peak heat release rate (HRR) versus K_2CO_3 and silica gel particle size. Within experimental uncertainty, K_2CO_3 and silica gel particle size do not change the effect of silica gel on the HRR.

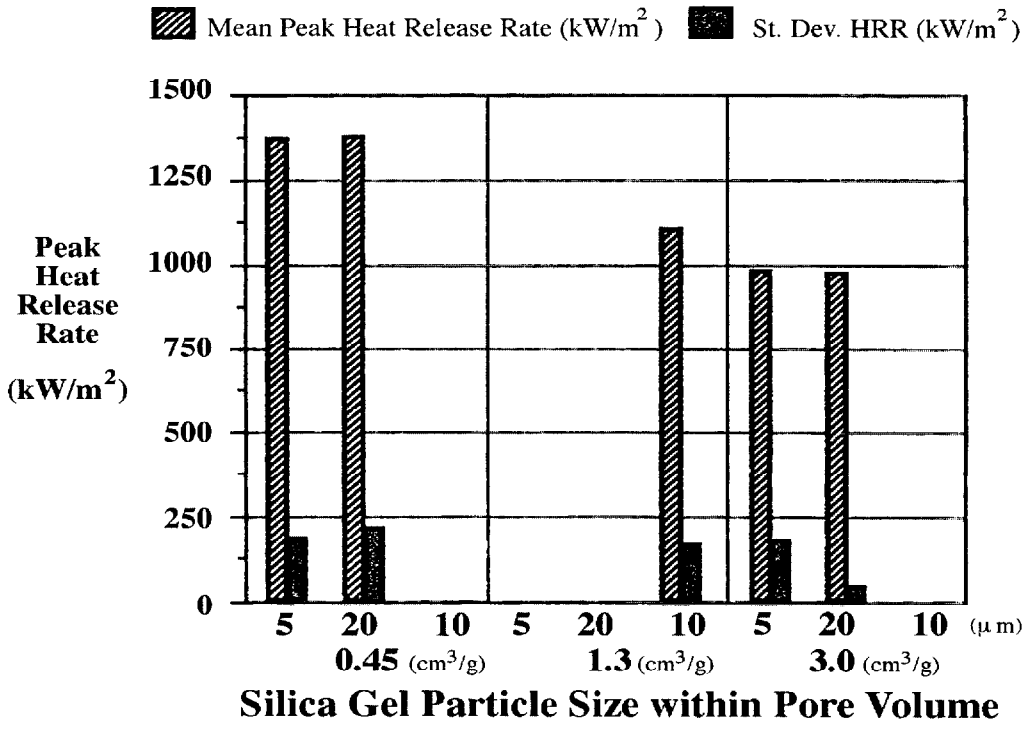

Figure 4. Peak HRR versus particle size and pore volume. Clearly, the pore volume has a strong influence on the reduction in HRR produced by the silica gels.

These data show that pore volume is, within experimental uncertainty, the primary factor in enhancing the fire retardant properties of silica gel in PP. The Cone Calorimetry data also shows that the high pore volume silica gel samples do not reduce flammability by changing the gas phase combustion processes, i.e., the carbon monoxide yield is unchanged (0.04 kg/kg ± 0.001 kg/kg) and, as Figure 6 shows, the specific heat of combustion, Hc, is unchanged as the pore volume is varied.

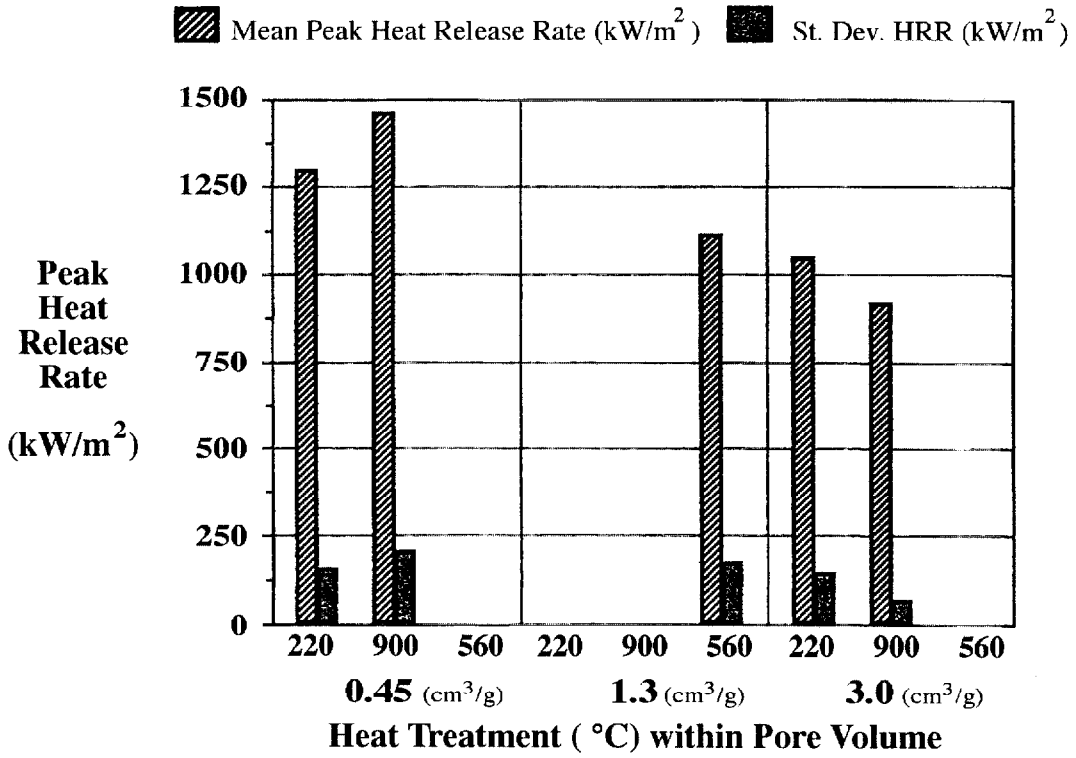

Figure 5. Peak HRR versus pore volume and heat treatment. This shows, again, that the pore volume has a strong affect on the reduction in HRR produced by the silica gels, and that the heat treatment of the silica gels does not appear to change their effectiveness.

Again, the silica gel particle size appears to have little influence on the effectiveness of the silica gel. Figure 5 shows that, within the experimental uncertainty, the heat treatment does not affect the flammability of the PP/silica gel formulations either.

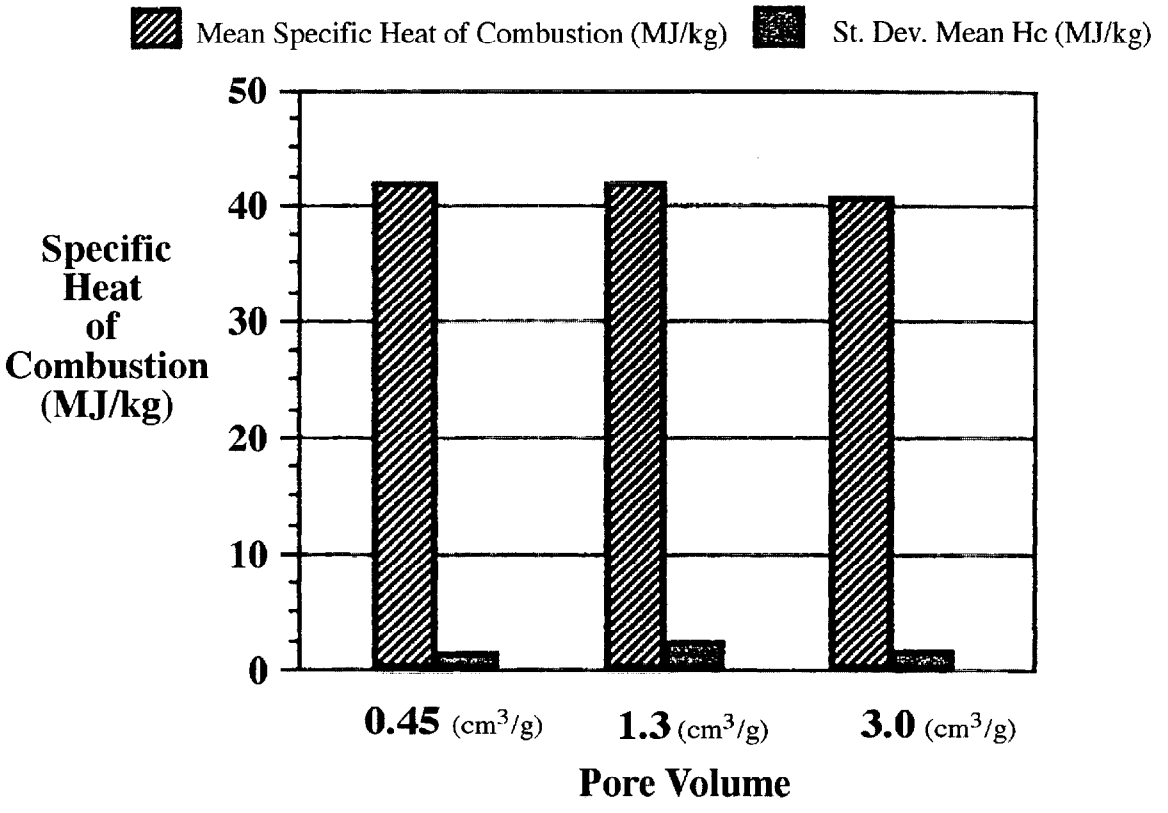

Figure 6. Specific heat of combustion (Hc) versus silica gel pore volume.

The silica gel appears to function by reducing the rate that fuel is fed into the gas phase. This can be seen by examining Figure 7, which shows the mass loss rate data for the three different pore volumes studied. One possible explanation for this behavior is that the larger pore diameter of the high pore volume silica gels can accommodate the PP macromolecule, or it's decomposition products. The radius of gyration of PP, in this molecular weight range, is ~70 nm, when measured in solution[7], and may be somewhat smaller in the melt. The nominal average pore diameter of the high pore volume material is ~28 nm. Since, there is a distribution of pore diameters it seems likely that a significant fraction of the pores might be able to fit a PP macromolecule, or it's decomposition products; thereby trapping or delaying the loss of decomposition products from the condensed phase, and thus reducing the mass loss rate.

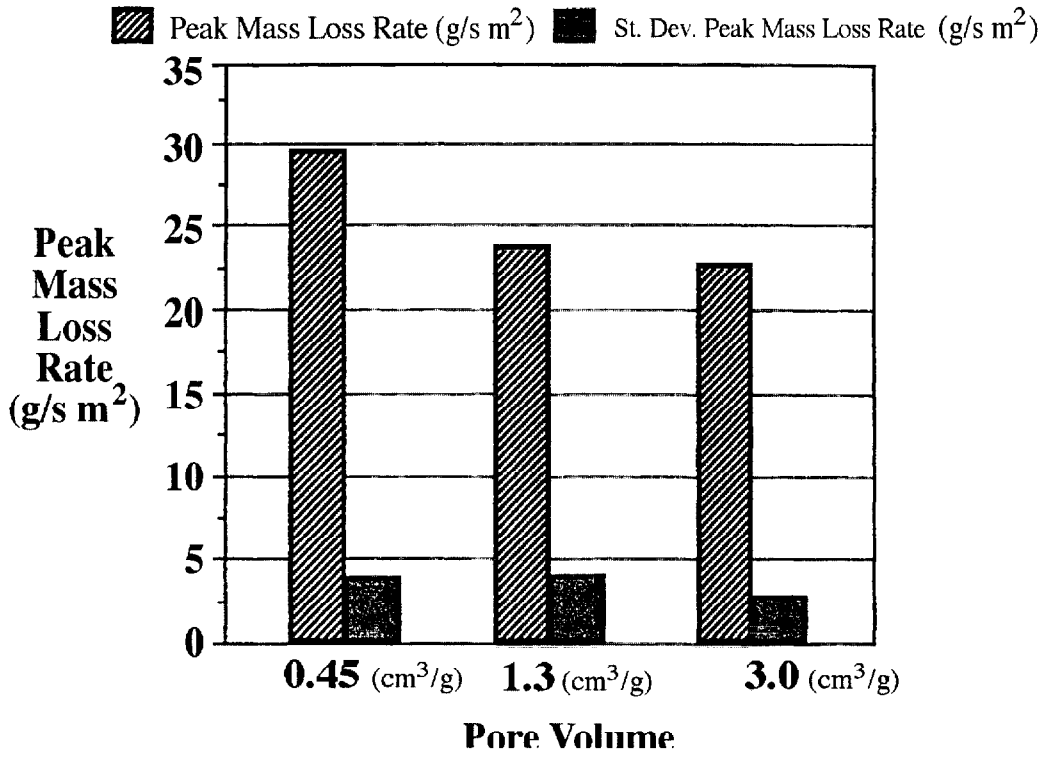

Figure 7. Mass loss rate data for the three different pore volumes studied.

In this phase of the flammability study of the FR properties of silica gel we have observed an enhanced effectiveness of the silica gel. The reduction in peak HRR compared to pure PP or (PP with PP-g-MA) is ~60% for the formulations with high pore volume silica gel. Figure 8 shows the HRR versus time plots for PP, PP/PP-g-MA with high pore volume (3.0 cm^3/g) silica gel and PP/PP-g-MA with the low pore volume (1.o cm^3/g) silica gel similar to that used in our original study.[2] These data show that the high pore volume silica gel is 2 times as effective as the original low pore volume material.

Two other important differences between the most recent results and our original results are apparent. First, in the results reported above, K_2CO_3 has little effect: Second, we obtained much lower (0 % to 4 mass %) carbonaceous char yields from the above samples, than in our original study (9 mass %). The reasons for the differences may be due to some subtle differences (processing, crystallinity, chain-branching, tacticity, additive or impurity) between the PP's used in the two cases.

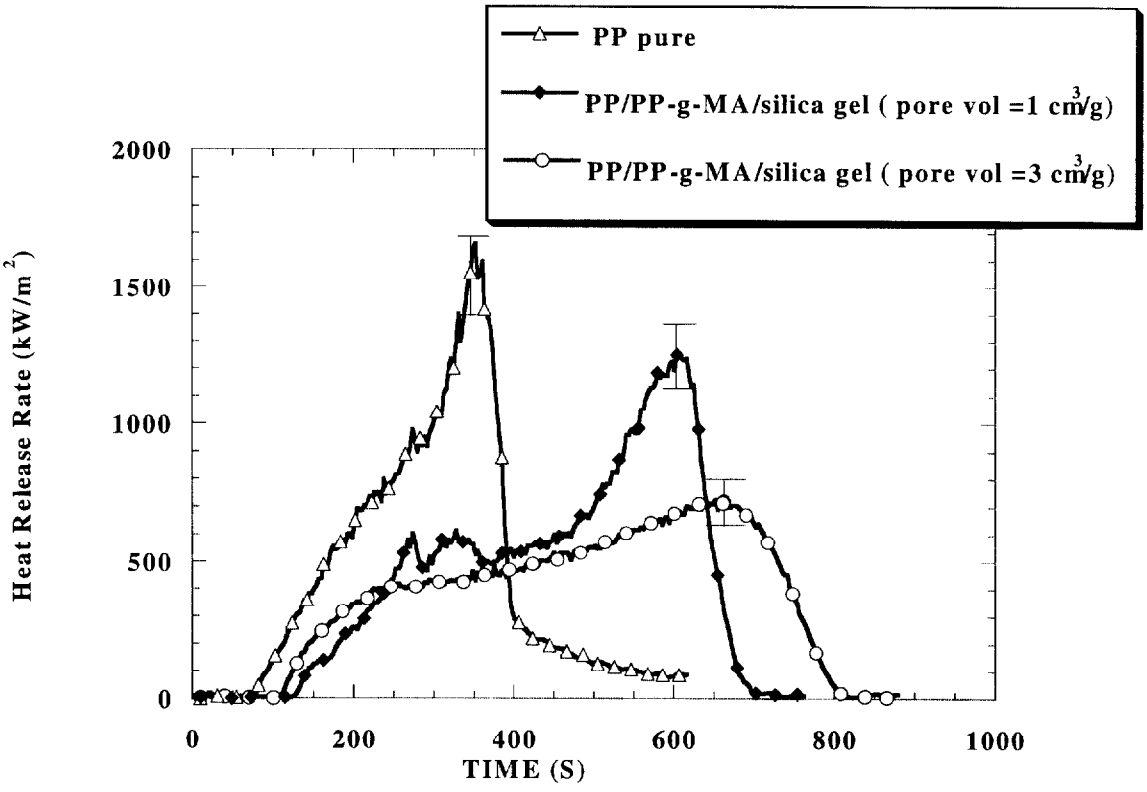

Figure 8. The HRR versus time plots for pure PP, PP/PP-g-MA (mass fraction 5%) with mass fraction 10 % high pore volume (3.0 cm^3/g) silica gel, and PP/PP-g-MA (mass fraction 5%) with mass fraction 10 % low pore volume (1.0 cm^3/g) silica gel.

Silica Gel, Fused Silica, and Fumed Silica.

To further explore the influence of silica material properties (morphology, surface area, silanol concentration, and surface treatment) on silica FR–properties, we prepared silica/PP samples using silicas with very different characteristics. We used fused silica, fumed silica, and a high pore volume (2.0 cm^3/g) silica gel. We used a 2.0 cm^3/g pore volume silica gel instead of the 3.0 cm^3/g since the former was easier to manufacture and gave identical effect on flammability properties. In contrast to the previous samples, which were mixed via extrusion, these samples were prepared by hand mixing powdered PP with the various silicas, followed by compression molding.

Table 3 shows the material properties of the four types of silica used. These silicas are very different, specifically in terms of their particle morphology, surface area, and level of silanol functionality. Figure 9 shows representations of the silica types. Fumed silica, shown on the right-side of Figure 9, has no pore structure. It is made of 0.2 μm – 0.3 μm long chains of nanometer size primary silica particles. The fumed silica is hydrophilic due to the significant silanol concentrations (3–4 SiOH/nm^2), on the primary particle surface, it has a surface area of 255 m^2/g. The hydrophobic-fumed silica (not shown) has a similar morphology, but has significant less silanol concentration (1- 2 SiOH / nm^2), on the primary particle surface, since many of the silanols have been "capped" with organo-slianes, and it has a surface area of 140 m^2/g. The silica gels, shown on the left side of Figure 9, are also made up of primary particles, however silica gels have internal pore structure, significant silanol concentration (0.4 SiOH / nm^2), and high surface area (400 m^2/g, 90 % of which is internal surface area). In silica gels the primary particles may be larger, and are extensively bridged, or crosslinked, to create pores. Finally, the fused silica, shown in the center of Figure 9, (made from melting, then cooling, and grinding amorphous, glass–sand) has no significant pore structure, low surface area, and very little silanol functionality.[8]

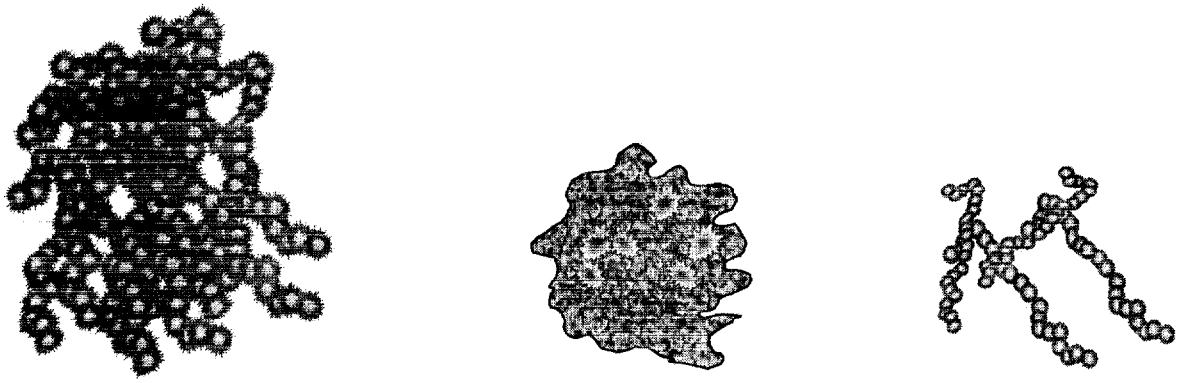

Figure 9. Drawing representing the different silica-morphologies for silica gel (left), fused silica (center), and fumed silica (right).

Table 3. Material properties of various silicas.

Silica	Porosity (cm^3/g)	Thermal Treatment (°C, h)	Silanol Density ($SiOH/nm^2$)	Surface Area (m^2/g)	Particle size (μm)
Fused Silica amorphous	~ 0	100 °C 2h	low	low	7
Fumed Silica hydrophilic	NA	None	3 - 4	255 ± 25	aggregate length 0.2 – 0.3
Fumed Silica hydophobic[a]	NA	100 °C 15h	1 - 2	140 ± 30	" "
Silica Gel	2.0	900 °C 15h	0.4	400 ± 40	17

a: ~ half of the SiOH groups are capped by trimethysilylation.[9]

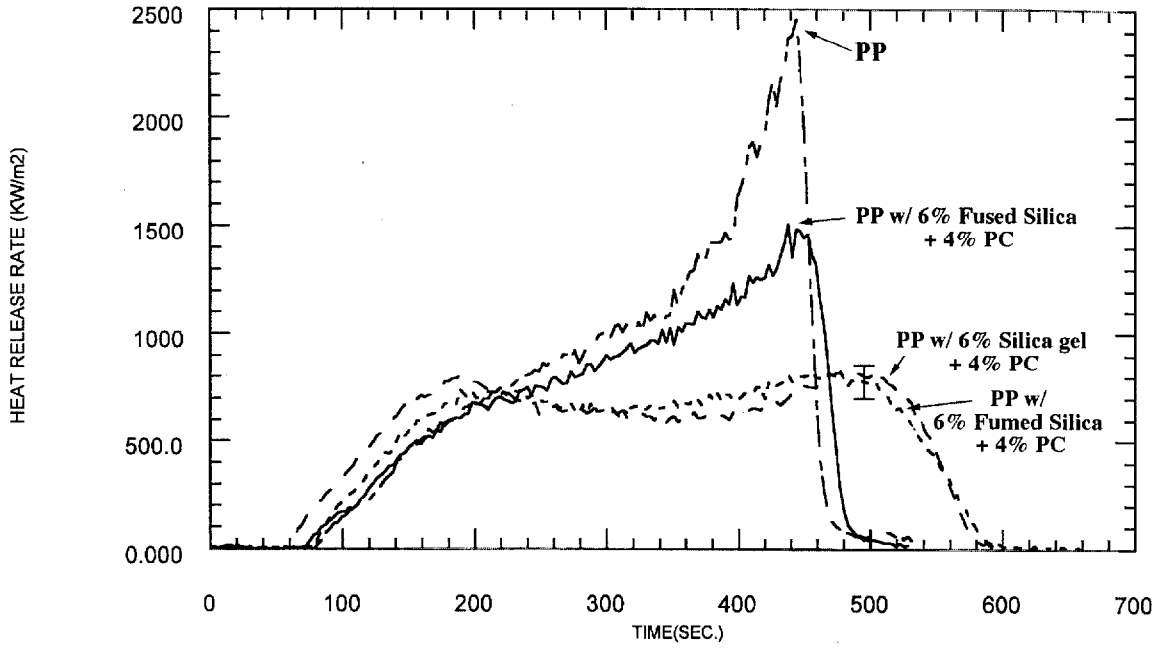

Figure 10. Heat release rate versus time plot of PP, PP w/ with mass fraction 6 % fused silica w/ mass fraction 4 % K_2CO_3 (PC), PP w/ with mass fraction 6 % fumed silica w/ mass fraction 4 % K_2CO_3 (PC), and PP w/ with mass fraction 6 % high pore volume silica gel w/ mass fraction 4 % K_2CO_3 (PC).

The Cone Calorimeter results, shown in Figure 10, reveal that the fused silica has only a moderate effect on the peak heat release rate of PP.[10] This may be because the fused silica has no pore structure. Also, Figure 10 reveals that hydrophilic fumed silica gives the same factor-of-3 reduction in peak heat release rate that large-pore silica gel produces. Since hydrophilic fumed silica has no pore structure this result challenges our proposed model for silica gel flammability reduction: i.e., where PP, or it's decomposition products are trapped in the larger pores, delaying the loss of decomposition products from the condensed phase, and thus reducing the mass loss rate.

3.2. Gasification Studies

An alternative FR mechanism for fumed silica may be related to the well-known thickening effect hydrophilic fumed silicas have on non-polar liquids.[13] When hydrophilic fumed silicas are suspended in non-polar liquids an inter-particle hydrogen-bonding network forms: this silica network increases the viscosity dramatically. Such an increase in the viscosity of the molten polymer during burning would reduce the rate of transport of volatile decomposition products through the molten layer, thus reducing the mass loss rate and the flammability.

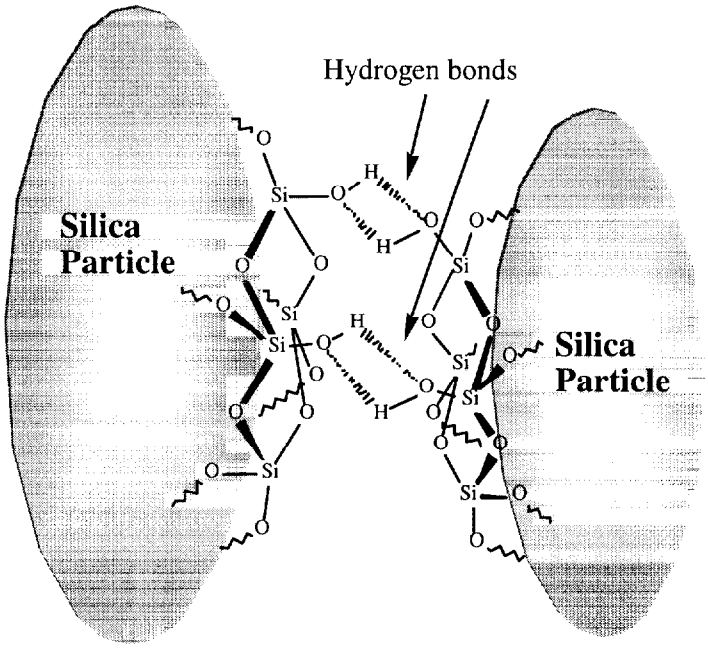

Figure 11. Inter-particle hydrogen bonding in hydrophilic fumed silica. This creates a hydrogen bonding network in a suspension of fumed silica in non-polar liquids.[9]

In order to confirm this hypothesis, and to understand the flame retardant mechanism of both the fumed silica and silica gels, the various types of silicas, shown in Table 3, were added to PP, and these samples were exposed to an external radiant flux in a nitrogen atmosphere using the gasification device shown previously in Figure 2. No gas phase oxidation reactions occur in the gasification device: therefore, the observed results are solely based on the chemical, and physical processes occurring in the condensed phase. There is no energy feedback from the flame to the sample: therefore, the energy input to the sample is well-defined by the external radiant flux, and its level is constant during the gasification test. (In the Cone Calorimeter, the energy flux to the sample consists of the external radiant flux (not absorbed by the flame), and the energy feedback from the flame. This value can change during the burning period, and can be different depending on whether the sample is flame retarded or not.)

Observation of the gasification of the unmodified PP sample first reveals melting of the sample surface at about 30 s after irradiation (heat flux: 40 kW/m^2), followed by the appearance of several large isolated bubbles at the surface, at about 60 s. Continued melting of the sample with more large bubbles was observed at about 90 s. Vigorous bubbling started at about 120 s and the sample surface was covered by a foamy-froth of very small bubbles (very similar in appearance to that of a beer "head") at about 180 s. This can be seen in the top left image in Figure 12. Vigorous bubbling, and a foamy-froth, continued over the rest of the gasification experiment as seen in the middle of the top image in Figure 12.

The digitized video images of the sample of PP with fused silica (mass fraction 10 %) are not shown in Figure 12, however, similar bubbling phenomena as that of pure PP sample was observed up to about 200 s. At about 250 s, the surface layer appeared to be more viscous, and had many small bubbles bursting through a more viscous, frothy-foam surface layer. This behavior continued until about 500 s when the surface became solid-like. Scattered white powder was observed after the end of the test, and its weight was close to 10 % of the original sample weight.

The digitized video images of the sample of PP with hydrophobic fumed silica (mass fraction 10 %) are also not shown in Figure 12; however, the behavior was similar to that of the pure PP sample up to about 200 s, with vigorous bubbling but without foaming, or any frothy-foam layer. After about 200 s, the sample had large bubbles rising through a viscous layer. However, this layer still looked like a fluid. After 400 s, some solid-looking islands were observed, and this pattern remained until the end of test. Vigorous bubbling was observed between the islands.

For the sample of PP with silica gel (mass fraction 10 %) initial melting and bubbling phenomena were similar to the above three samples up to about 180 s, as seen in the left bottom picture in Figure 12. At about 180 s, the sample

surface rapidly solidified and a crust-like layer formed. It appeared that this layer continued to thicken; the production of the evolved degradation products slowed significantly, as seen in the middle and right bottom images in Figure 12. It appeared that molten polymer below the crust was transported to the surface through the crust by capillary action. The mass of the residue at the end of the test (800 s) appeared to be a rigid crust instead of a powder, and was about 9% of the original sample mass. Although the color of the residue was light gray, it appears that no significant amount of carbonaceous char was formed by the addition of the silica gel. Behavior very similar to the PP/silica gel sample was also observed for the PP/hydrophilic fumed silica sample: except that the surface layer of the residue at the end of the test was very fluffy and white.

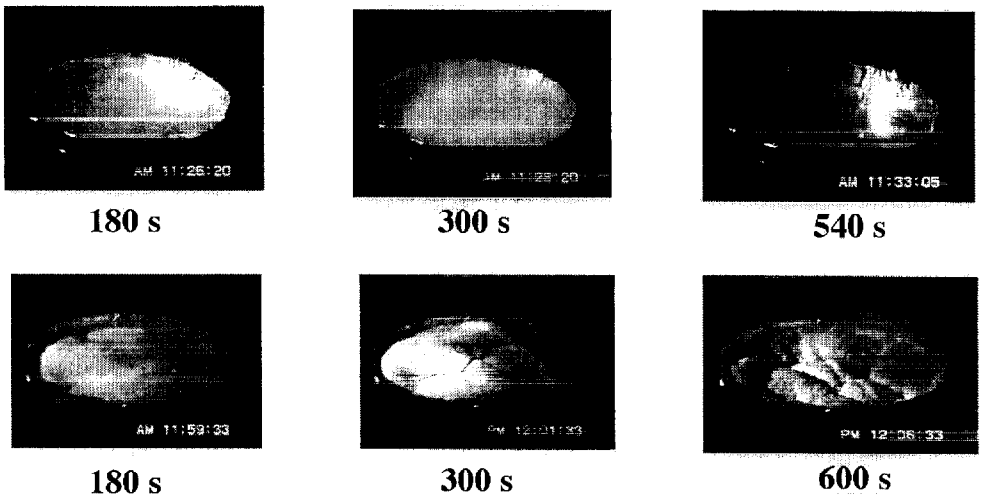

Figure 12. Digitized images of sample surface during gasification in N_2 at 40 kW/m^2. Pure PP (Top row) ; PP with silica gel (mass fraction 10 %) (bottom row).

The measured mass loss rates of the five samples are shown in Figure 13. A sharp increase in mass loss rate after about 200 s is clearly seen for the pure PP sample. After 300 s, the mass loss rates of the modified samples decrease in the order: PP/fused silica > PP/ hydrophobic fumed silica > PP/silica gel • PP/hydrophilic fumed silica. However, the mass loss rates of all samples are nearly the same until about 220 s. Actually, the addition of the four silicas slightly increases the mass loss rate before 200 s. This could be due to increased radiation absorptivity of the samples due to the strong broad band absorption of Si-O peak at about 1100 cm^{-1}, as described later. This tends to absorb the external radiation close to the sample surface, and thus heats the sample surface faster.

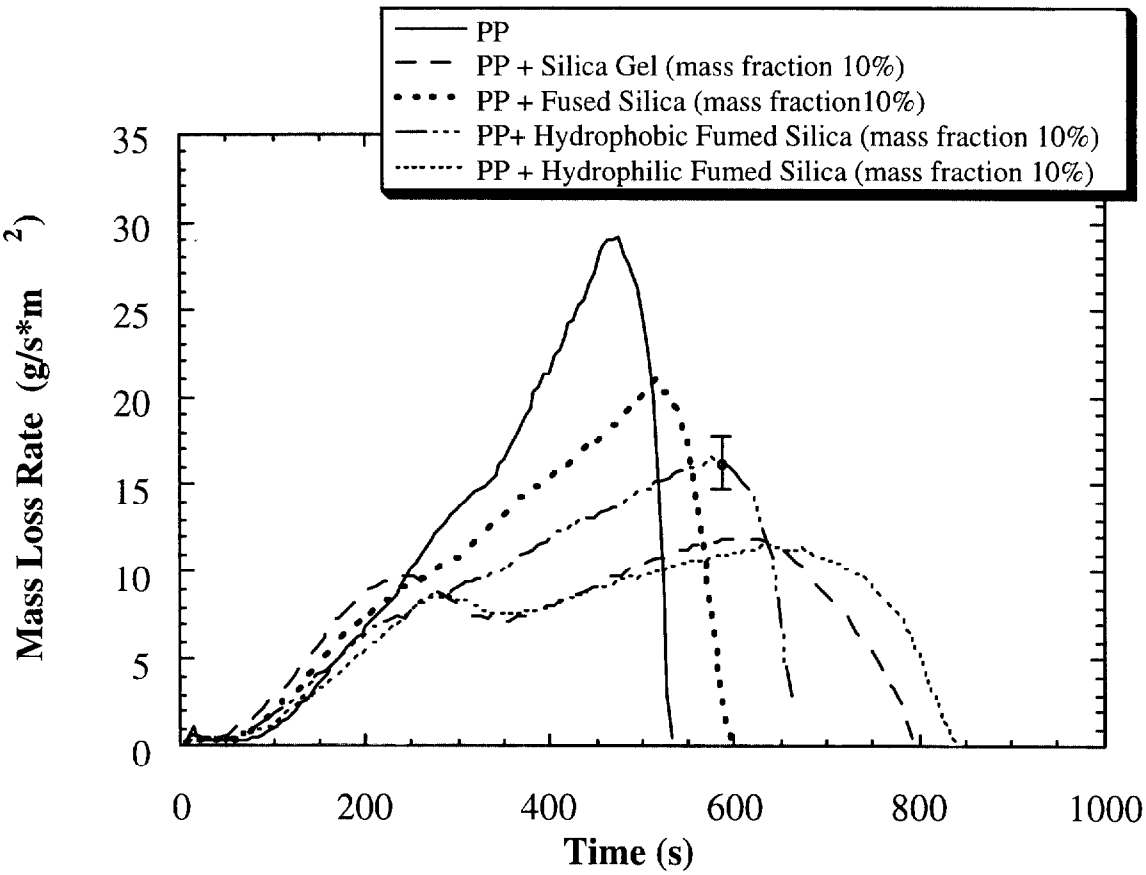

Figure 13. The mass loss rate data from the gasification (N_2 at 40 kW/m^2) of: pure PP, PP/silica gel, PP/fused silica, PP/hydrophobic fumed silica, and PP/hydrophilic fumed silica. This shows the effect of silica type on the gasification rate of PP.

From the visual observations of the gasification experiments it appears that the melt viscosity of PP is significantly enhanced by the addition of silica. Both silica gel and hydrophilic fumed silica show the same thickening behavior; with hydrophobic fumed silica and fused silica showing only slight thickening. For the hydrophilic fumed silica the thickening is due to the inter-particle hydrogen bonding shown in Figure 11; on the other hand, the thickening from silica gel can in part be due to this type of mechanism, but entanglement of the polymer in the large silica gel pores may also play a part in increasing the viscosity. [11]

After the formation of the crust layer, molten polymer and degradation products may seep through the crust layer toward the surface by capillary action. However, this transport rate through the crust layer tends to be much slower than transport by bubble formation/movement through the more viscous molten layer in the pure PP sample.

The same types of PP samples were tested in the Cone Calorimeter to examine the effect of each silica (except for the hydrophilic fumed silica) on heat release rate and mass loss rate during burning. The heat release rate results are shown in Figure 14; mass loss rate results are shown in Figure 15. Although the external heat flux used in the Cone Calorimeter was 35 kW/m^2, instead of 40 kW/m^2 as in the gasification device, the relative order of mass loss rate among the four samples is exactly the same as that shown in Figure 13. Heat release rate and mass loss rate decrease in the order: pure PP > PP/fused silica > PP/ hydrophobic fumed > PP/silica gel.

Comparison of the mass loss rate between the Cone Calorimeter and the radiative gasification device indicates that the mass loss rates observed in the Cone Calorimeter are about 10 % – 15% higher than those in the gasification device in spite of higher external flux in the gasification experiment. This is due to the energy feedback from the flame to the sample in the Cone Calorimeter. Heat release rates and mass loss rates for the samples with the silicas are slightly higher than that of pure PP before ~ 200 s. This trend was also observed in the gasification device.

Therefore, the comparison of the results obtained in the two cases, one without combustion in nitrogen, and the other with combustion, indicates that the addition of the silicas to PP affects the condensed phase processes instead of gas phase processes.

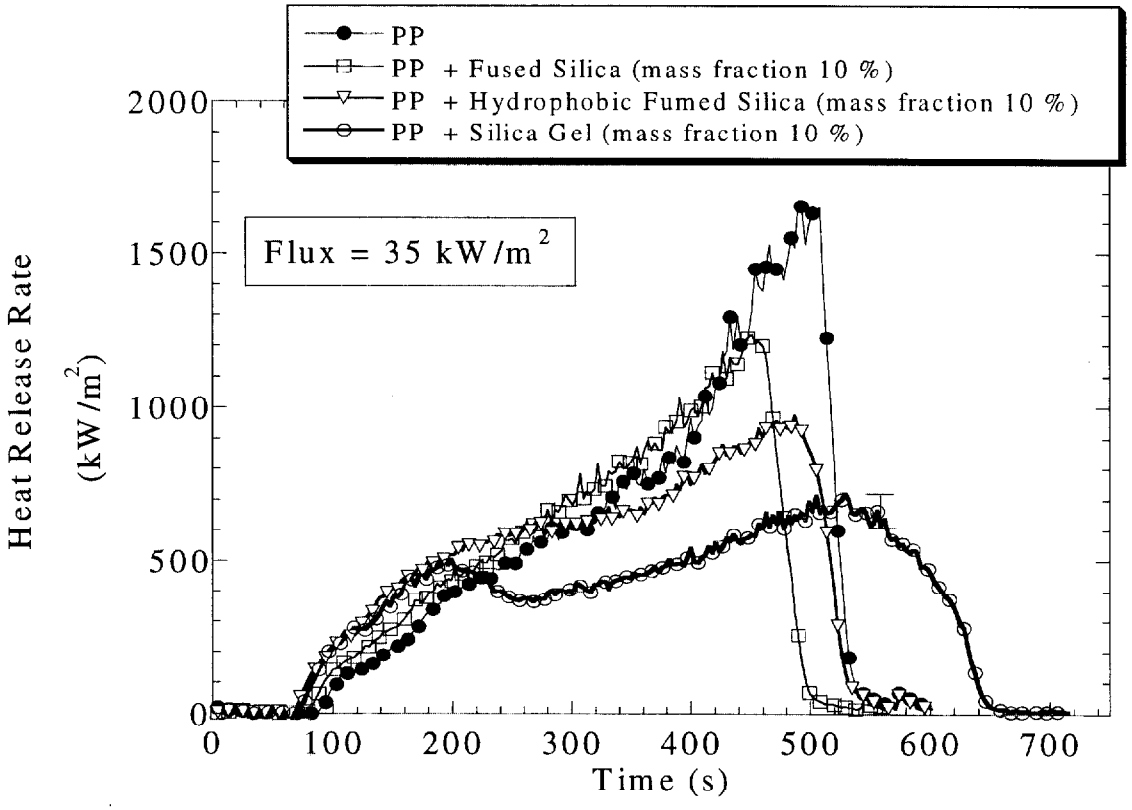

Figure 14. Heat release rate plot of: pure PP, PP with fused silica (mass fraction 10 %), PP with silica gel (mass fraction 10 %), and PP with hydrophobic fumed silica (mass fraction 10 %).

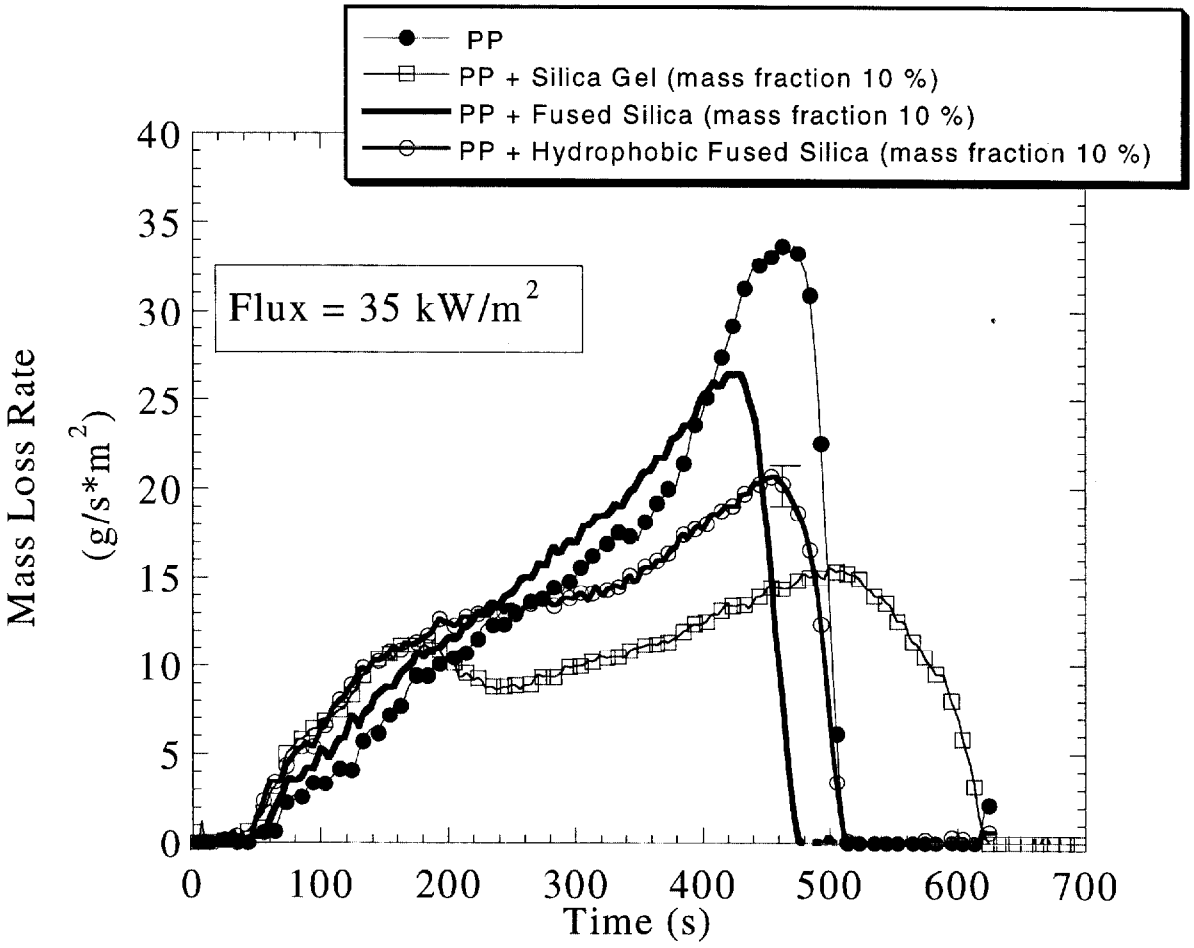

Figure 15. Mass loss rate plot (during burning) of: pure PP, PP with fused silica (mass fraction 10 %), PP with silica gel (mass fraction 10 %), and PP with hydrophobic fumed silica (mass fraction 10 %).

The above trends indicate that the FR mechanism of silicas tends to be physical in nature, instead of chemical. In order to confirm this hypothesis, gasification sample residues were collected at 300 s into a typical gasification experiment. This was done to examine the chemical changes in the sample due to pyrolysis. The absorption spectra of the original and heat exposed samples of PP with silica gel were obtained by FTIR analysis (KBr pellets). A comparison of the spectra for an unheated sample, and the residue from a sample irradiated in nitrogen, shown in Figure 16, indicates that no new peaks (bonds) were formed during the gasification.

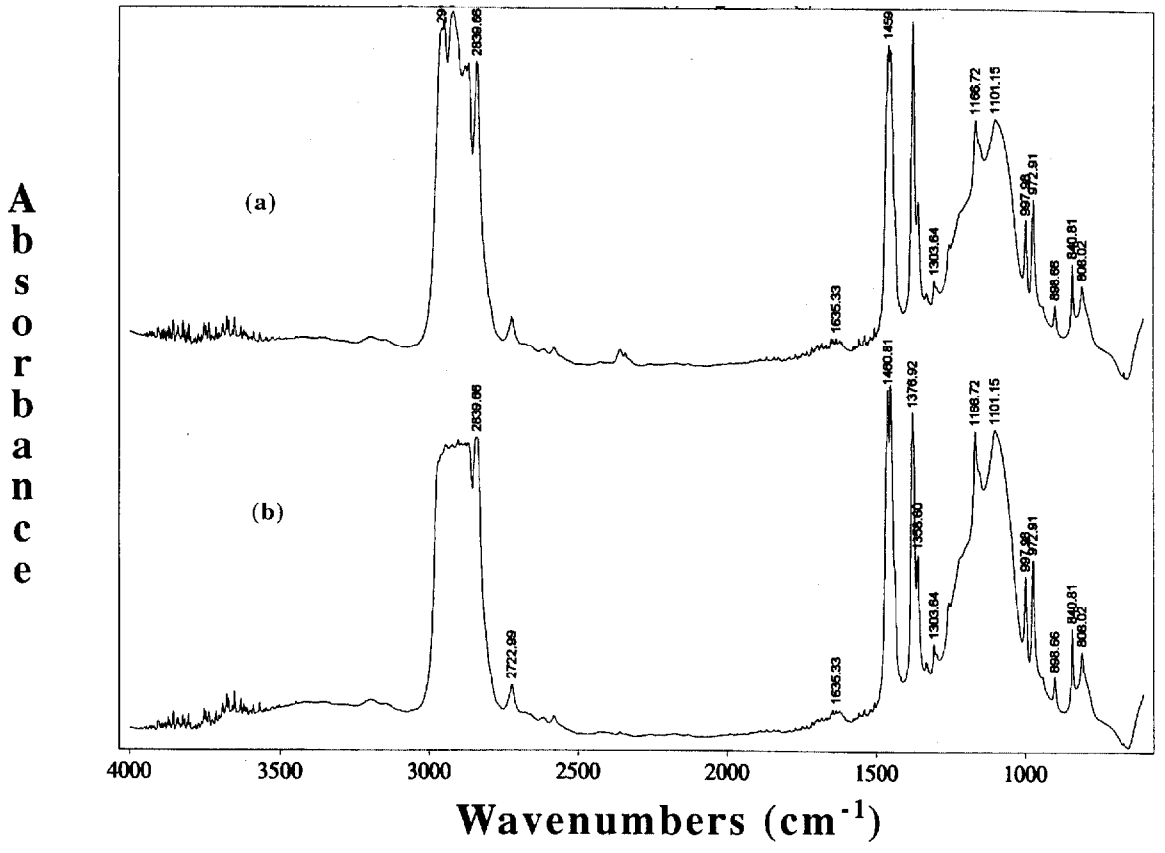

Figure 16. Comparison of FTIR spectra of PP with silica gel (mass fraction 10%) un-pyrolysed (a) and pyrolysed (b).

Some of the peaks in the spectra are identified in Table 4.

Table 4. FTIR data and assignments for untreated and pyrolized samples of: pure PP and PP with silica gel.

IR absorbance	Assignment
2940 cm^{-1} to 2840 cm^{-1}	C-H stretching
doublet at ~ 1460 cm^{-1}	bending of CH_2 and CH_3 (splitting due to crystallinity)
~ 1378 cm^{-1}	CH_3 symmetric deformation
~ 1167 cm^{-1}	helix deformation in crystalline phase of PP
~ 1100 cm^{-1}	Si-O-Si stretching
~ 998 cm^{-1} and 973 cm^{-1}	helical segments in the amorphous phase of PP
899 cm^{-1}	unidentified peak
~ 840 cm^{-1} and 808 cm^{-1}	skeletal backbone PP vibration

All these peaks appear in both the original and residue samples. This further confirms that the affects of silica on mass loss rate of PP, are mainly physical, condensed phase processes, instead of chemical ones.

To attempt to determine why the silica gel FR effect does not start until 200 s into the Cone or gasification tests, we evaluated the accumulation of silica at the PP sample surface during a typical gasification test. This was accomplished by measurement of the silicon concentration at the top layer of residues collected at different times. Five samples were collected: unheated, 185 s, 300 s, 500 s, and 875 s. The silicon concentration in the collected samples was measured by neutron activation analysis at Dow Chemical Company. The results are shown in Figure 17, with the corresponding mass loss rate curve. The trend of the measured silicon concentration agrees reasonably well with the mass loss rate curve: a higher rate of increase in silicon concentration corresponds to a higher rate of increase in the mass loss rate, and a lower rate when the mass loss rate decreases, except at the end of the test. The increase in Si concentration at the sample surface is caused by accumulation of silica gel during continued degradation and gasification of PP. The silicon concentration in the sample increased about ten times from the initial value, and it is expected that the residue consists mainly of silica at the end of test: because no char formation is observed. The weight of the residue at the end of the test was about 8 % to 9 % of the original weight so it appears that a small fraction of silica gel might be carried away into the gas phase during the tests.[12] With an increase in Si concentration at the sample surface, melt viscosity of the mixture of PP and silica gel increases dramatically during the progress of the gasification, thus the surface becomes a solid crust-like layer, as described above.

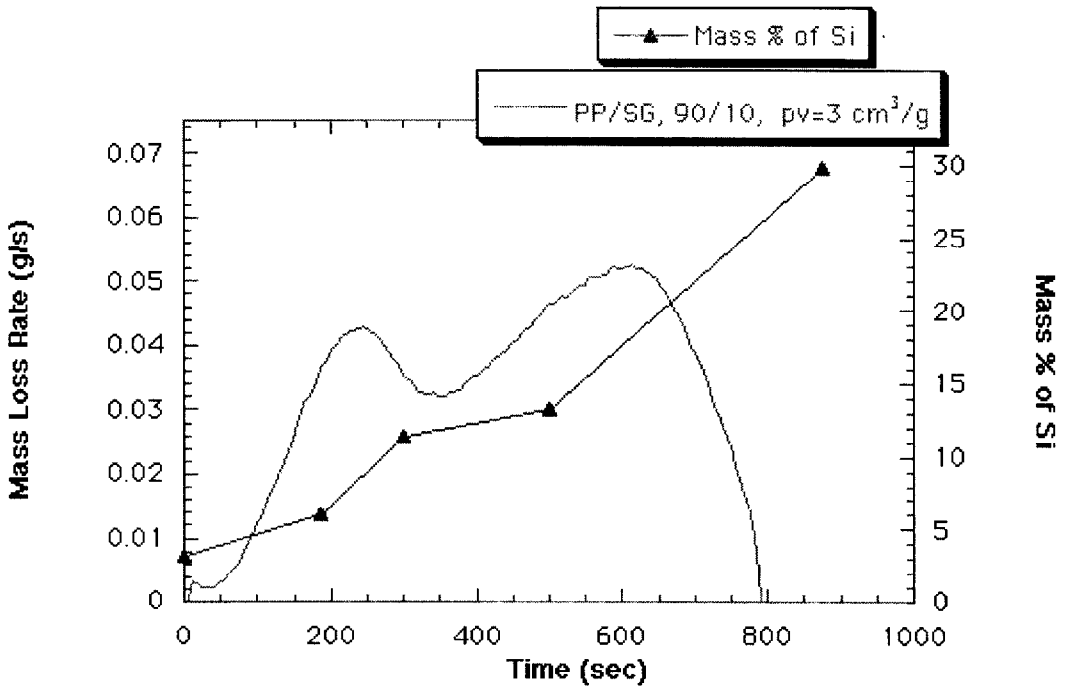

Figure 17. Mass loss rate and Si surface concentration data from the gasification, in N_2 at 40 kW/m^2, of PP with silica gel (mass fraction 10 %). This data shows the direct relationship between the mass loss rate and Si concentration at the surface.

The basis for the physical effect of silica may be due to the thermal properties of the silica-loaded crust layer. The thermal diffusivities of accumulated silica gel, and of PP, are estimated here. The thermal conductivity[9] of silica varies significantly depending on its porosity. For example, it is 0.015 W/mK for fumed silica, and 1.1 W/mK for fused silica. Here the thermal conductivity of silica gel is assumed to be close to that of fumed silica. The estimated thermal diffusivity of the silica gel is roughly 1 x 10^{-4} cm^2/s compared to 6 x 10^{-2} cm^2/s for PP. Although, the value for silica gel is estimated, it is clear that the thermal diffusivity of the silica loaded crust layer should be much less than that of PP. Furthermore, the insulating effect of this layer should improve as the test progresses. The thermal diffusivity of fused silica is about the same as that of PP; therefore we assume that the addition of fused silica to PP does not have any significant effect on the thermal diffusivity of PP.

The reduction in the transport rate of thermal degradation products through the molten polymer layer, due to an increase in melt viscosity by the accumulation of fused silica, could explain the difference in mass loss rate between PP and PP/fused silica, shown in Figure 13. However, since no crust-like layer forms due to the accumulation of fused silica, the increase in melt viscosity appears to be much less than that from fumed silica or silica gel. The difference in mass loss rate between PP/hydrophilic fumed silica and PP/hydrophobic fumed silica, shown in Figure 13, is due to the greater increase in viscosity of PP melt by hydrophilic fumed silica as compared to hydrophobic fumed silica, and thus a greater reduction in the transport rate of the degradation products in PP/ hydrophilic fumed silica. Therefore, the silica gel flame retardant mechanism in PP appears to consists of two mechanisms: first, reduction in the transport rate of the thermal degradation products; and second, reduction in thermal diffusivity of the sample near the surface due to gradual accumulation of silica gel, which acts as a thermal insulation layer. This is also true for fumed silica. The reduction in the transport rate of the degradation products is achieved by dramatically increasing the viscosity of PP melts due to hydrogen bonding of hydroxyl groups of silanols, and entanglement of polymer chains with the large pores of silica gel. This transport mechanism tends to dominate early in the test, because a small amount of silanol increases melt viscosity dramatically,[13] but the insulation mechanism requires a relatively large accumulation of fumed silica, or silica gel, for the layer to become an effective insulator.

3.3. Ethylene Vinyl Acetate Copolymer

It is known that hydrogen bonding of silica particles via surface-silanols occurs in non-polar fluids, and that in polar fluids the inter-particle hydrogen bonds are disrupted, and any thickening effect is attenuated. Therefore, the addition of silica gel to *polar* polymers may not significantly increase their melt viscosity, due to the lack of inter-particle hydrogen bonding. Consequently, the observed reduction in the mass loss rate of polar polymers, by the addition of silica gel, would be due mainly to the above described insulation effect of the accumulated silica gel layer. In order to test this hypothesis, EVA (19 % vinyl acetate), was selected as the polar polymer. EVA and several other additives were tested in addition to silica gel; they were fused silica, K_2CO_3, and melamine polyphosphate, MPP. The latter two additives were selected to explore synergism between with silica gel and these additives.

Gasification rates for pure EVA, and EVA with silica gel (mass fraction 10 %) were measured in nitrogen at 40 kW/m^2 in the gasification device. Melting and vigorous bubbling were observed during gasification of the pure EVA sample. For the EVA / silica gel sample, melting and vigorous bubbling were observed up to about 160 s, followed by the formation of a surface layer which erupted occasionally with large bubbles evolved from below the surface. Solidification and the formation of the crust layer were observed at about 250 s, but many cracks formed throughout the crust layer. Cracks may have formed due to the use of thin sample thickness (0.3 cm for the EVA samples compared to 0.8 cm for the PP samples). The mass loss rate results are shown in Figure 18. Although the mass loss rate of the EVA / silica gel sample is lower than that of EVA: the reduction in mass loss rate is not as large as we observed for PP. The solidification observed early in the PP / silica gel experiments, did not occur for the EVA/ silica gel sample. The observed formation of the surface layer after 160 s appears to be due to accumulation of silica gel; the difference in mass loss rate between the pure EVA, and the EVA / silica gel sample, is due to the insulating effect of the accumulated silica gel layer. This confirms the above described mechanism.

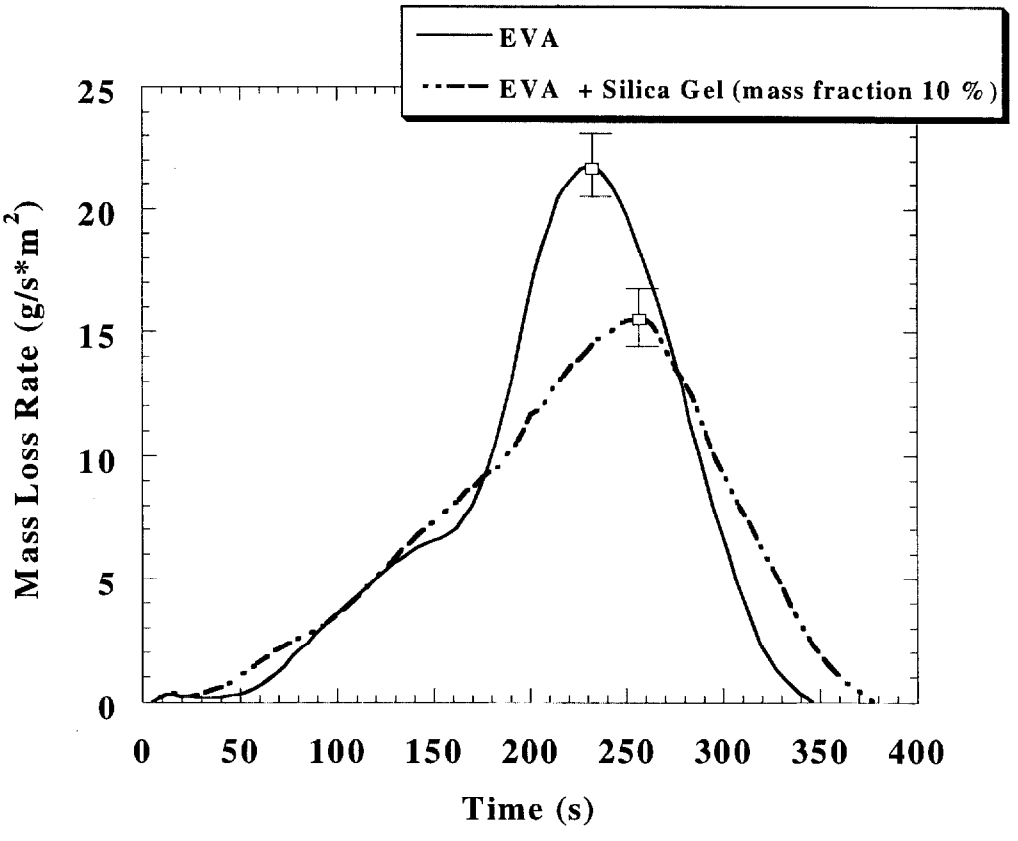

Figure 18. Mass loss rate data from the gasification, in N_2 at 40 kW/m^2, of pure EVA, and EVA with silica gel (mass fraction 10 %).

Figure 19 and Figure 20 show the heat release rate and mass loss rate data, respectively, for the five EVA samples measured at an external radiant flux of 35 kW/m^2 in the Cone Calorimeter. The results indicate that the addition of silica gel significantly reduces heat release rate and mass loss rate of EVA, as effectively as that observed for PP. Ignition delay time was shortened significantly and heat release rate (also mass loss rate) at the early stage was increased for the silica gel, silica gel with potassium carbonate, and for the silica gel with MPP. The addition of fused silica does not have any significant effect on heat release rate and mass loss rate of EVA. No significant synergism was observed between silica gel and potassium carbonate, or between silica gel and melamine polyphosphate.[14] The addition of potassium carbonate along with silica gel actually increased heat release rate and mass loss rate starting at 205 s.

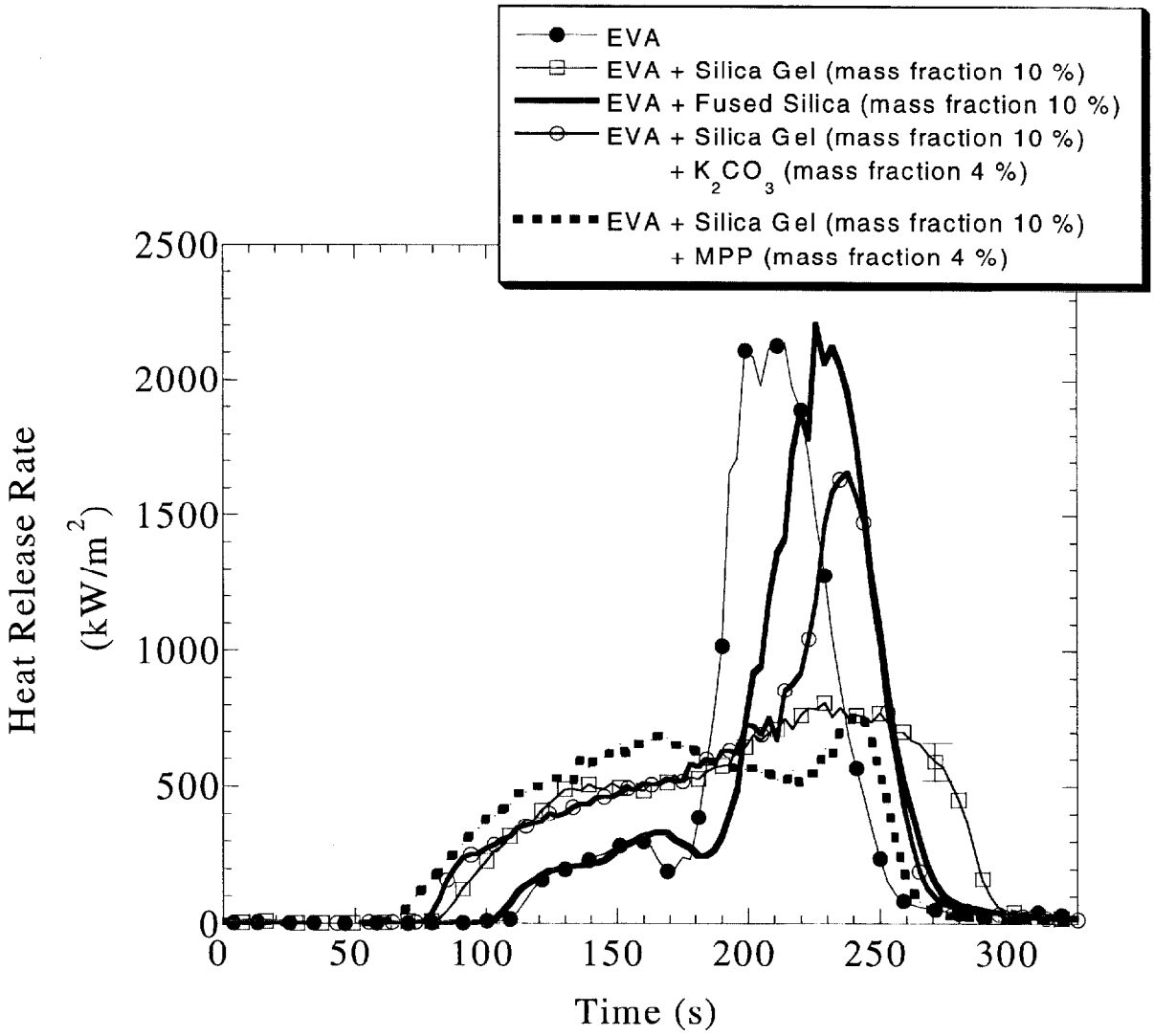

Figure 19. HRR plots for EVA, EVA with fused silica (mass fraction 10 %), EVA with silica gel (mass fraction 10 %), EVA with silica gel (mass fraction 6 %) and K_2CO_3 (mass fraction 4 %), EVA with silica gel (mass fraction 6 %) and MPP (mass fraction 4 %).

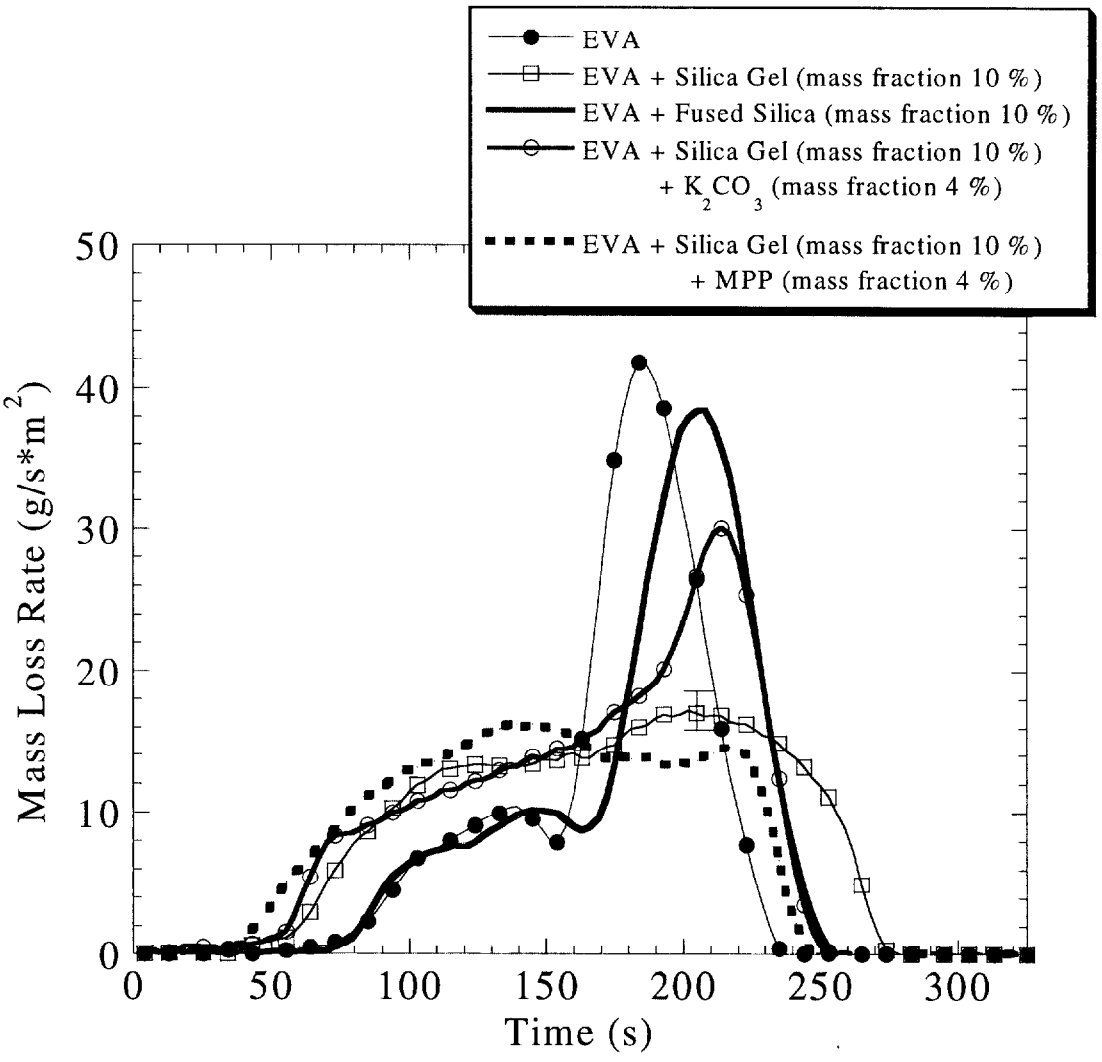

Figure 20. Mass loss rate plots measured in the Cone Calorimeter for EVA, EVA with fused silica (mass fraction 10 %), EVA with silica gel (mass fraction 10 %), EVA with silica gel (mass fraction 6 %) and K_2CO_3 (mass fraction 4 %), EVA with silica gel (mass fraction 6 %) and MPP (mass fraction 4 %).

The results obtained in the Cone Calorimeter show much larger reduction in mass loss rate for the EVA / silica gel sample, compared with pure EVA, than that observed in the gasification study in nitrogen. During the burning test of the EVA / silica gel sample, in the Cone Calorimeter, the formation of a thin solid surface layer appeared at an early stage of the test. Recall that this did not happen in the gasification experiment. In the Cone Calorimeter experiment this layer could be formed by an oxidation reaction with air during the pre-ignition pyrolysis period. This layer could be acting as a barrier to slow down the transport rate of degradation products to the gas phase, or as an insulation layer. However, such a layer was not observed for pure EVA. Although it is not clear what oxidative reaction occurred for the EVA / silica gel sample, it appears that a chemical mechanism is possible by the addition of silica gel to certain polar polymers such as EVA, which is not observed with non-polar polymer such as PP. The study will continue to pursue this issue further as a part of an in-house project.

4. SUMMARY

We propose that the silica FR mechanism is comprised of two main effects: first, reduction in the transport rate of the thermal degradation products by a dramatic increase in the viscosity of the polymer melt; this is due to hydrogen bonding of silanol groups, and entanglement of polymer chains within the large pores of silica gel; and second, reduction in thermal diffusivity of the sample near the surface, due to gradual accumulation of silica, which acts as a thermal insulation layer. The relative contribution of each of these effects depends on the physical properties and morphology of the silicas, as well as the polar nature of the polymers used.

5. ACKNOWLEDGEMENTS

The authors would like to thank the members of the New Flame Retardants Consortium: The PQ Corporation, Nyacol Products, Inc., FMC Corporation, Sekisui America Corporation, and AKZO NOBEL for support of this work. We also thank Dow Chemical Corporation for Si analysis. We would also like to thank Mr. Michael Smith for Cone Calorimeter analysis, Mr. Randy Shields for performing gasification experiments, Dr. Ed Weil and Dr. Bob Patterson for helpful suggestions, and Ms. Lori Brassell for sample preparation and analysis.

6. REFERENCES

[1] Kashiwagi, T., Gilman, J. in "Polymer Flammability and Flame Retardants" (see Silicon Based Flame Retardants chapter), eds, Wilkie, C., Grand, A., in press.

[2] Gilman, J., Ritchie, S., Kashiwagi, T., and Lomakin, S., *Fire and Materials*, vol 21, 23-32, (1997).

[3] J. Gilman, T. Kashiwagi, S. Lomakin, D. L. VanderHart and V. Nagy, "Characterization of Flame Retarded Polymer Combustion Chars by Solid-State ^{13}C and ^{29}Si NMR and EPR," Fire and Materials: 22, 61-67, (1998).

[4] According to ISO 31-8, the term "Molecular Weight" has been replaced by "Relative Molecular Mass", symbol M_r Thus, if this nomenclature and notation were used here, $M_{r,n}$ instead of the historically conventional M_n for the average molecular weight (with similar notation for M_w, M_z, M_v) would be used. It would be called the "Number Average Relative Molecular Mass". The conventional notation, rather than the ISO notation, has been employed here.

[5] Samples were also made (by injection molding) into 75 mm by 4 mm, 18 g disks. No difference, within experimental uncertainty, in their flammability, due to the different sample shape and density was observed.

[6] Babraukus, V., Peacock, R., *Fire Safety Journal*, 18 (1992) 255.

[7] Polymer Handbook, eds. J. Brandrup, E.H. Immergut, John Wiley & Sons, Inc., V24, Second Edition, 1975.

[8] KAPOLITE Inc. Siltex, Fused Silica, Data sheet.

[9] G. Wypych, Handbook of Fillers, 2nd Edition, Chemical Technology Publishing, Toronto, Canada, Chapter 2, 1999.

[10] After these experiments were performed we found that the K_2CO_3 was not needed.

[11] R.K. Iler, The Chemistry of Silica, John Wiley & Sons, New York, p. 588 (1979).

[12] There is some discrepancy in the Si concentration values in Figure 17. The initial mass percent should be about 4.5 % for 10 % loading of silica gel in PP, instead of the measured value of 3.2 % ± 0.3 %; furthermore, at the end of the test, the Si concentration should be close to 45 % (assuming all silica) instead of the measured value of 29.8 % ± 0.9 %. Although it is not clear what caused this discrepancy, the observed trend shown in the figure is quite reasonable.

[13] "CAB-O-SIL Untreated Fumed Silica Properties and Functions" Cabot Corp. TD-100, May (1997).

[14] The same result was found in another set of experiments done for this program exploring MPP as a synergist for silicas in PP.

NIST-114 (REV. 6-93) ADMAN 4.09

U.S. DEPARTMENT OF
NATIONAL INSTITUTE OF STANDARDS AND TECHNOLOGY

MANUSCRIPT REVIEW AND APPROVAL

(ERB USE ONLY)	
ERB CONTROL NUMBER: G	DIVISION:
PUBLICATIONS REPORT NUMBER: No.	CATEGORY CODE:
PUBLICATION DATE:	NO. PRINTED PAGES:

INSTRUCTIONS: ATTACH ORIGINAL OF THIS FORM TO ONE (1) COPY OF MANUSCRIPT AND SEND TO: WERB SECRETARY, BUILDING 820, ROOM 125

TITLE AND SUBTITLE (CITE IN FULL)

New Flame Retardants Consortium: Final Report: Flame Retardant Mechanism of Silica

CONTRACT OR GRANT NUMBER

TYPE OF REPORT AND/OR PERIOD COVERED

AUTHOR(S) (LAST NAME, FIRST INITIAL, SECOND INITIAL)

Jeffrey W. Gilman, Takashi Kashiwagi, Marc Nyden, Richard H. Harris, Jr.

PERFORMING ORGANIZATION (CHECK (X) ONE BOX)

- [X] NIST/GAITHERSBURG
- [ ] NIST/BOULDER
- [ ] NIST/JILA

LABORATORY AND DIVISION NAMES (FIRST NIST AUTHOR ONLY)

Building and Fire Research Laboratory, Fire Science Division

SPONSORING ORGANIZATION NAME AND COMPLETE ADDRESS (STREET, CITY, STATE, ZIP)

PROPOSED FOR NIST PUBLICATION

- [ ] JOURNAL OF RESEARCH (NIST JRES)
- [ ] J. PHYS. & CHEM. REF. DATA (JPCRD)
- [ ] HANDBOOK (NIST HB)
- [ ] SPECIAL PUBLICATION (NIST SP)
- [ ] TECHNICAL NOTE (TN)
- [ ] MONOGRAPH (NIST MN)
- [ ] NATL. STD. REF. DATA SERIES (NIST NSRDS)
- [ ] FEDERAL INFO. PROCESS. STDS. (NIST FIPS)
- [ ] LIST OF PUBLICATIONS (NIST LP)
- [X] INTERAGENCY/INTERNAL REPORT (NISTIR)
- [ ] LETTER CIRCULAR
- [ ] BUILDING SCI. SERIES
- [ ] PRODUCT STANDARDS
- [ ] OTHER
- [ ] —

PROPOSED FOR NON-NIST PUBLICATION (CITE FULLY): [ ] —U.S. FOREIGN— [ ]

Fire and Materials Journal

PUBLISHING MEDIUM:	X	PAPER		DISKETTE		CD-ROM		WWW		OTHER

SUPPLEMENTARY NOTES

ABSTRACT (A 2000-CHARACTER OR LESS FACTUAL SUMMARY OF MOST SIGNIFICANT INFORMATION. IF DOCUMENT INCLUDES A SIGNIFICANT BIBLIOGRAPHY OR LITERATURE SURVEY, CITE IT HERE. SPELL OUT ACRONYMS ON FIRST REFERENCE.) (CONTINUE ON SEPARATE PAGE, IF NECESSARY.)

The results of a two year research project carried out with the "New Flame Retardants Consortium" are reported. This investigation into the flame retardant mechanism of silica gel and other forms of silica has determined that the silica FR mechanism is comprised of two main effects. The first is a reduction in the transport rate of the thermal degradation products by dramatically increasing the viscosity of the polymer melt due to hydrogen bonding of surface silanol groups and entanglement of polymer chains within the large pores of silica gel. Second is the reduction in thermal diffusivity of the sample near the surface due to gradual accumulation of silica, which acts as a thermal insulation layer.

KEY WORDS (MAXIMUM OF 9; 28 CHARACTERS AND SPACES EACH; SEPARATE WITH SEMICOLONS; ALPHABETIC ORDER; CAPITALIZE ONLY PROPER NAMES)

fire retardant; halogen-free; silica;

AVAILABILITY:

- [X] UNLIMITED
- [ ] FOR OFFICIAL DISTRIBUTION - DO NOT RELEASE TO NTIS
- [ ] ORDER FROM SUPERINTENDENT OF DOCUMENTS, U.S. GPO, WASHINGTON, DC 20402
- [X] ORDER FROM NTIS, SPRINGFIELD, VA 22161

NOTE TO AUTHOR(S); IF YOU DO NOT WISH THIS MANUSCRIPT ANNOUNCED BEFORE PUBLICATION, PLEASE CHECK HERE. [ ]